Inverted polymer solar cells with amorphous indium zinc oxide as the electron-collecting electrode

Hyeunseok Cheun,[1] Jungbae Kim,[1] Yinhua Zhou,[1] Yunnan Fang,[2] Amir Dindar,[1] Jaewon Shim,[1] Canek Fuentes-Hernandez,[1] Kenneth H. Sandhage,[2] and Bernard Kippelen[1,*]

[1]*School of Electrical and Computer Engineering and Center for Organic Photonics and Electronics, 777 Atlantic Dr., Atlanta, GA 30332, (U.S.A.)*
[2]*School of Materials Science and Engineering, 777 Atlantic Dr., Atlanta, GA 30332, U.S.A.*
**kippelen@ece.gatech.edu*

Abstract: We report on the fabrication and performance of polymer-based inverted solar cells utilizing amorphous indium zinc oxide (*a*-IZO) as the electron-collecting electrode. Amorphous IZO films of 200 nm thickness were deposited by room temperature sputtering in a high-purity argon atmosphere. The films possessed a high optical transmittance in the visible region (≥ 80%), a low resistivity (3.3×10^{-4} Ωcm), a low surface roughness (root mean square = 0.68 nm), and a low work function (4.46 ± 0.02 eV). Inverted solar cells with the structure *a*-IZO/P3HT: PCBM/PEDOT:PSS/Ag exhibited a power conversion efficiency of 3% estimated for AM 1.5G, 100 mW/cm^2 illumination.

OCIS codes: (350.6050) Solar energy; (040.5350) Photovoltaics; (230.0250) Optoelectronics; (310.6860) Thin films, optical properties; (310.7005) Transparent conductive coatings

References and Links

1. B. Kippelen, and J. L. Bredas, "Organic photovoltaics," Energy Environ. Sci. **2**(3), 251–261 (2009).
2. C. J. Brabec, "Organic photovoltaics: technology and market," Sol. Energy Mater. Sol. Cells **83**(2-3), 273–292 (2004).
3. S. R. Forrest, "The path to ubiquitous and low-cost organic electronic appliances on plastic," Nature **428**(6986), 911–918 (2004).
4. S. K. Hau, H. L. Yip, N. S. Baek, J. Y. Zou, K. O'Malley, and A. K. Y. Jen, "Air-stable inverted flexible polymer solar cells using zinc oxide nanoparticles as an electron selective layer," Appl. Phys. Lett. **92**(25), 253301 (2008).
5. Y. H. Zhou, H. Cheun, W. J. Potscavage, Jr., C. Fuentes-Hernandez, S. Kim, and B. Kippelen, "Inverted organic solar cells with ITO electrodes modified with an ultrathin Al2O3 buffer layer deposited by atomic layer deposition," J. Mater. Chem. **20**(29), 6189–6194 (2010).
6. C. Waldauf, M. Morana, P. Denk, P. Schilinsky, K. Coakley, S. A. Choulis, and C. J. Brabec, "Highly efficient inverted organic photovoltaics using solution based titanium oxide as electron selective contact," Appl. Phys. Lett. **89**(23), 233517 (2006).
7. M. S. White, D. C. Olson, S. E. Shaheen, N. Kopidakis, and D. S. Ginley, "Inverted bulk-heterojunction organic photovoltaic device using a solution-derived ZnO underlayer," Appl. Phys. Lett. **89**(14), 143517 (2006).
8. T. Kuwabara, Y. Kawahara, T. Yamaguchi, and K. Takahashi, "Characterization of Inverted-Type Organic Solar Cells with a ZnO Layer as the Electron Collection Electrode by ac Impedance Spectroscopy," ACS Appl Mater Interfaces **1**(10), 2107–2110 (2009).
9. J. W. Kang, W. I. Jeong, J. J. Kim, H. K. Kim, D. G. Kim, and G. H. Lee, "High-performance flexible organic light-emitting diodes using amorphous indium zinc oxide anode," Electrochem. Solid-State Lett. **10**(6), J75–J78 (2007).
10. Y. S. Park, K. H. Choi, and H. K. Kim, "Atmospheric Plasma Treatment of Flexible IZO Electrode Grown on PET Substrate for Flexible Organic Solar Cells," Electrochem. Solid-State Lett. **12**(12), H426–H429 (2009).
11. S. H. Han, Y. H. Kim, S. H. Lee, M. H. Choi, J. Jang, and D. J. Choo, "Stable organic thin-film transistor in a pixel for plastic electronics," Org. Electron. **9**(6), 1040–1043 (2008).
12. J. B. Kim, C. Fuentes-Hernandez, S. J. Kim, S. Choi, and B. Kippelen, "Flexible hybrid complementary inverters with high gain and balanced noise margins using pentacene and amorphous InGaZnO thin-film transistors," Org. Electron. **11**(6), 1074–1078 (2010).
13. B. Yaglioglu, Y. J. Huang, H. Y. Yeom, and D. C. Paine, "A study of amorphous and crystalline phases in In2O3-10wt.% ZnO thin films deposited by DC magnetron sputtering," Thin Solid Films **496**(1), 89–94 (2006).

#133177 - $15.00 USD Received 10 Aug 2010; revised 9 Sep 2010; accepted 10 Sep 2010; published 17 Sep 2010

14. T. Sasabayashi, N. Ito, E. Nishimura, M. Kon, P. K. Song, K. Utsumi, A. Kaijo, and Y. Shigesato, "Comparative study on structure and internal stress in tin-doped indium oxide and indium-zinc oxide films deposited by r.f. magnetron sputtering," Thin Solid Films **445**(2), 219–223 (2003).
15. Y. S. Park, H. K. Kim, S. W. Jeong, and W. J. Cho, "Highly flexible indium zinc oxide electrode grown on PET substrate by cost efficient roll-to-roll sputtering process," Thin Solid Films **518**(11), 3071–3074 (2010).
16. T. J. Marks, J. G. C. Veinot, J. Cui, H. Yan, A. Wang, N. L. Edleman, J. Ni, Q. Huang, P. Lee, and N. R. Armstrong, "Progress in high work function TCO OLED anode alternatives and OLED nanopixelation," Synth. Met. **127**(1-3), 29–35 (2002).
17. Y. Gassenbauer, and A. Klein, "Electronic surface properties of rf-magnetron sputtered In2O3: Sn," Solid State Ion. **173**(1-4), 141–145 (2004).
18. A. Klein, C. Korber, A. Wachau, F. Sauberlich, Y. Gassenbauer, R. Schafranek, S. P. Harvey, and T. O. Mason, "Surface potentials of magnetron sputtered transparent conducting oxides," Thin Solid Films **518**(4), 1197–1203 (2009).
19. R. Martins, P. Almeida, P. Barquinha, L. Pereira, A. Pimentel, I. Ferreira, and E. Fortunato, "Electron transport and optical characteristics in amorphous indium zinc oxide films," J. Non-Cryst. Solids **352**(9-20), 1471–1474 (2006).
20. H. C. Pan, M. H. Shiao, C. Y. Su, and C. N. Hsiao, "Influence of sputtering parameter on the optical and electrical properties of zinc-doped indium oxide thin films," J. Vac. Sci. Technol. A **23**(4), 1187–1191 (2005).
21. M. Glatthaar, M. Niggemann, B. Zimmermann, P. Lewer, M. Riede, A. Hinsch, and J. Luther, "Organic solar cells using inverted layer sequence," Thin Solid Films **491**(1-2), 298–300 (2005).
22. H. Cheun, C. Fuentes-Hernandez, Y. H. Zhou, W. J. Potscavage, Jr., C. Fuentes-Hernandez, S. Kim, J. Shim, D. Amir, and B. Kippelen, "Electrical and optical properties of ZnO processed by atomic layer deposition in Inverted polymer solar cells," J. Phys. Chem. C. submitted.

1. Introduction

Lightweight polymer-based solar cells with potentially low-cost processability could open up and impact consumer markets as a renewable energy solution [1–3]. Recently, inverted solar cells with a transparent electron-collecting electrode have been demonstrated [4,5]. These cells exhibited improved air stability with similar power conversion efficiencies as solar cells with a conventional architecture (i.e., for which the device is fabricated on top of a hole-collecting electrode). Inverted polymer solar cells using indium tin oxide (ITO) as the bottom electron-collecting electrode generally required an additional surface modification with a thin buffer layer of TiO_x, ZnO, or Al_2O_3 to lower the work function [5–7]. ITO modifications with metal oxides can also require UV treatment or applying constant forward bias to increase electrical conductivity [5,8]. Hence, there is a need for transparent electron-collecting electrodes of low work function that can be used in solar cells with an inverted structure without the need for a series of modifications involving additional processing steps.

Amorphous transparent conducting oxides (*a*-TCOs) have been used as electrodes or semiconducting layers in a variety of optoelectronic devices, such as light-emitting diodes [9], solar cells [10], and organic [11] or oxide [12] thin-film transistors. Owing to a high conductivity, high optical transparency, and the capability for processing at low temperature with low surface roughness and low residual internal stresses, amorphous indium zinc oxide (*a*-IZO) can be an attractive *a*-TCO [13–15]. These characteristics enable the incorporation of *a*-IZO in the fabrication of polymer solar cells on plastic substrates. Amorphous IZO films with a high work function (5.2 eV) have been used as hole-transporting electrodes [9,16]. However, the direct use of *a*-IZO as an *electron-collecting electrode* in inverted polymer solar cells requires a significant modification of its work function. In the past, it has been reported that the position of the Fermi level in several TCOs can be raised by increasing the oxygen (O_2) partial pressure in the gas atmosphere used during sputtering [17,18]. Conversely, by reducing the oxygen partial pressure in the sputtering atmosphere, the position of the Fermi level may be lowered with a corresponding reduction in the work function.

In this work, we report on the structural, optical, electrical, and surface properties of an *a*-IZO layer deposited by radio-frequency (RF) sputtering in a high-purity argon (Ar) atmosphere at room temperature (RT). Amorphous IZO films deposited in this low O_2 atmosphere exhibited a low work function (4.46 eV), which enables the direct use of such films as electron-collecting electrodes in inverted polymer solar cells. Here, we demonstrate the fabrication and performance of inverted polymer solar cells utilizing an *a*-IZO layer as an electron-collecting electrode. Inverted solar cells with the structure

#133177 - $15.00 USD Received 10 Aug 2010; revised 9 Sep 2010; accepted 10 Sep 2010; published 17 Sep 2010

a-IZO/P3HT:PCBM/PEDOT:PSS/Ag reach power conversion efficiencies of 3% estimated for AM 1.5G, 100 mW/cm^2 illumination, which is comparable with the performance of reference devices with the structure ITO/ZnO/P3HT:PCBM/PEDOT:PSS/Ag.

2. Experiment

To evaluate the structural, optical, electrical, and surface properties of the IZO film, 200-nm-thick IZO films were deposited on glass by RF sputtering at RT using a power of 150 W and a working pressure of 6 mTorr in a high-purity Ar atmosphere. An IZO target with 3 inch diameter and 0.125 inch thickness (10 wt % ZnO-doped In_2O_3, LTS Chemical Inc.) was used for sputtering. The oxygen content of the Ar exiting the sputtering chamber was measured to be ≤ 1.1 ppm with a gas sensor (OG-120M oxygen analyzer, Oxy-Gon Industries, Inc.). X-ray diffraction (XRD) analyses of IZO films on glass substrates were conducted with Cu Kα radiation using an X-Pert Pro Alpha 1 diffractometer and an X'Celerator linear detector (PANalytical, Almelo, The Netherlands). Optical transmission spectra of IZO films on glass substrates were obtained using a UV–Vis spectrometer (Cary 5E, Varian, Inc.) and a reference glass substrate. The refractive index of IZO films with thicknesses in the range from 125 to 300 nm deposited on SiO_2/Si substrates was measured by spectroscopic ellipsometry (M-2000 Ellipsometer, J. A. Woollam Co., Inc.) operating in reflection mode. The work function of IZO films on glass substrates was measured in air using a Kelvin Probe (Kelvin probe S, Besocke Delta Phi). A highly oriented pyrolytic graphite (HOPG) sample with a work function of 4.5 eV was used as the reference. The values of resistivity and sheet resistance of IZO films on glass substrates were obtained by the transmission line method (TLM). Atomic force microscopic (Dimension 3100 MultiMode AFM, NanoScope III controller, Veeco) images of IZO films on glass substrates were generated under atmospheric conditions.

Inverted polymer solar cells were fabricated on patterned *a*-IZO on glass substrates using blends of the donor polymer poly(3-hexylthiophene) (P3HT-4002E, Rieke Metals, Inc.) with the acceptor [6,6]-phenyl C_{61} butyric acid methyl ester (PCBM, Nano-C) as an active layer. ZnO-modified ITO films on glass substrates were used in reference devices. These reference films consisted of a 20-nm-thick ZnO layer deposited on an ITO substrate (Colorado Concept Coatings LLC) by atomic layer deposition (Savannah S100, Cambridge NanoTech) at 200 °C. The substrates were cleaned sequentially in an ultrasonic bath of deionized water, acetone, and isopropanol. P3HT:PCBM films were spin-coated on the *a*-IZO and ITO/ZnO substrates for 1 min at 700 rpm from a solution comprised of a mixture of P3HT and PCBM in chlorobenzene (P3HT:PCBM weight ratio = 1:0.7; total P3HT + PCBM concentration = 34 mg/ml). The solution was filtered through 0.2-μm-pore PTFE filters prior to spin-coating, and the resulting samples were annealed at 160 °C for 10 min in a nitrogen-atmosphere glove box. PEDOT:PSS (CPP 105 DM, H.C. Starck) was then spin-coated on top of the active layer at 5,000 rpm for 1 min in air, followed by annealing at 120 °C for 10 min in the glove box. A thin (150 nm) layer of Ag was then applied on the PEDOT: PSS layer by thermal evaporation at a rate of 0.1 – 0.3 nm and a base pressure of 2×10^{-7} Torr. The active device area was 0.1 cm^2. Current-voltage characteristics were measured using a source meter (Model 2400 SourceMeter, Keithley Instruments, Inc.) controlled by a LabVIEW program. For illumination, an AM1.5G solar simulator (Model 91160 Solar Simulator, Oriel Instruments) with an irradiance of I_L = 100 mW/cm^2 was used in the glove box. A monochromator coupled to a 175 W Xenon lamp (ASB-XE-175EX, CVI) and a calibrated photodiode (S2386-44K, Hamamatsu) were used to measure the external quantum efficiency (EQE).

3. Results and discussion

Figure 1a reveals XRD data that demonstrates the amorphous nature of the 200-nm-thick IZO films, both in the as-deposited state and after annealing at 160 °C (the annealing temperature

#133177 - $15.00 USD Received 10 Aug 2010; revised 9 Sep 2010; accepted 10 Sep 2010; published 17 Sep 2010

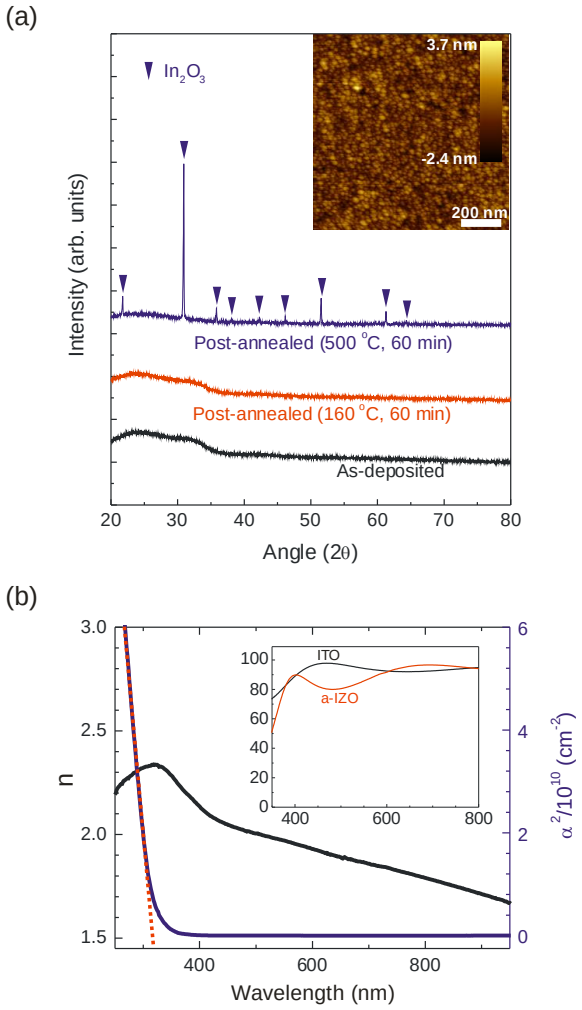

Fig. 1. (a) XRD patterns of the IZO film (200-nm-thick) deposited by RF sputtering and post-annealed at various temperatures for 60 min in air. Inset: AFM image (1 × 1 μm^2) of the *a*-IZO (200-nm-thick) film deposited at RT. (b) The real component of the refractive index and the square of the absorption coefficient (α) of *a*-IZO. Inset: Optical transmittance spectra of an *a*-IZO (200-nm-thick) and an ITO (150-nm-thick) films.

of the P3HT:PCBM layer in devices) for 60 min. Figure 1a also shows that annealing at 500 °C for 60 min resulted in appreciable crystallization of the IZO film. The inset of Fig. 1b presents optical transmittance spectra for a 200-nm-thick *a*-IZO and a 150-nm-thick ITO films. Figure 1b shows the real component of the refractive index and the square of the absorption coefficient (α) measured on *a*-IZO films. The optical properties of *a*-IZO were thickness independent. The linear dependence at the edge of the absorption band in the α^2-versus-wavelength plot indicates that electron momentum was largely conserved, so that the *a*-IZO films can be described by a direct-band-gap model with a bandgap energy of 3.94 eV (315 nm). Hence, the *a*-IZO films were transparent throughout the visible region. Such a large optical band gap is comparable with values reported for highly conductive IZO films [19,20]. TLM measurements yielded a resistivity value of 3.3×10^{-4} Ωcm and an average sheet resistance of about 18 Ω/□ in 200-nm-thick *a*-IZO films. Such a low value is comparable to

#133177 - $15.00 USD Received 10 Aug 2010; revised 9 Sep 2010; accepted 10 Sep 2010; published 17 Sep 2010

the value of commercial ITO (15 Ω/□ at a thickness of 150 nm). AFM analysis was conducted prior to application of the active layer. An AFM image of the *a*-IZO film is shown in the inset of Fig. 1a. The surface roughness (root mean square, RMS) of the *a*-IZO film was measured to be only 0.68 nm, which was significantly lower than that of the ITO/ZnO film (2.41 nm).

Kelvin probe measurements of *a*-IZO deposited on a glass substrate in the low- O_2, Ar-based atmosphere yielded work function values of 4.46 ± 0.02 eV in air. The lower values of these work functions, relative to values reported in the literature [9,16], may be attributed to a reduction in the effective Fermi level position due to suppression of the O_2 content during sputtering. To confirm this O_2-based effect, an *a*-IZO film was prepared by RF sputtering in an atmosphere of Ar mixed with O_2 at a volume ratio of Ar/O_2 = 96/4. The work function of this Ar/O_2-deposited film was found to be 4.74 ± 0.04 eV. These results indicate that the work function of *a*-IZO films can be modified by controlling the O_2 content during film deposition.

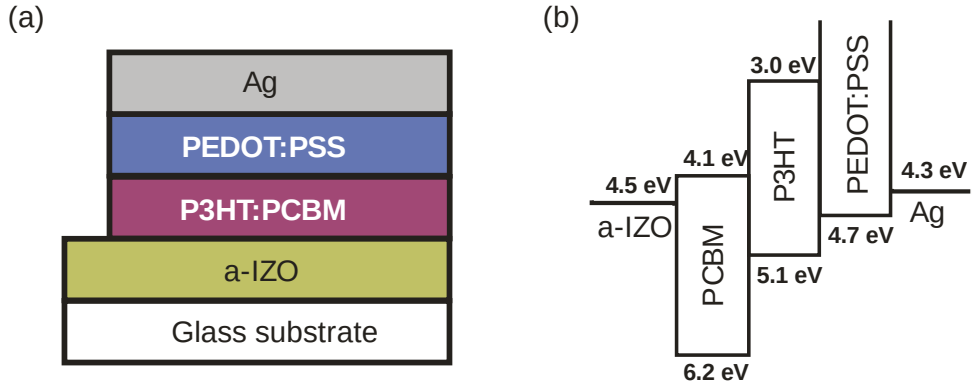

Fig. 2. (a) Device structure of an inverted P3HT:PCBM solar cell with an *a*-IZO electrode. (b) Energy level diagram of the components of the device.

The high optical transmittance in the visible region, the low resistivity, the low surface roughness, and the low work function make these *a*-IZO films excellent candidates for replacing modified-ITO electrodes in inverted polymer solar cells. To verify that *a*-IZO films can operate as transparent electrodes without the need of an additional buffer layer, inverted polymer solar cells were fabricated with the structure: *a*-IZO/P3HT:PCBM/PEDOT:PSS/Ag (Fig. 2a). Figure 2b illustrates the energy band diagram expected for this solar cell structure. The values for the energy level diagram have been taken from the literature [7,21]. The photovoltaic performance of these inverted devices was compared with those of reference devices using ITO/ZnO, with a work function of 4.33 ± 0.02 eV, as a transparent electron-collecting electrode. Figure 3a reveals the *J-V* characteristics measured on both inverted solar cell devices.

Table 1. Average[a] device performance of inverted devices with the structures of *a*-IZO/P3HT:PCBM/PEDOT:PSS/Ag and ITO/ZnO/P3HT:PCBM/PEDOT:PSS/Ag.

	V_{OC} (mV)	J_{SC} (mA/cm^2)	*FF*	*PCE* (%)	*Corrected (%)*[b]	*PCE*
a-IZO	588 ± 7	8.58 ± 0.15	0.62 ± 0.02	3.11 ± 0.12	2.90 ± 0.11	
ITO/ZnO	572 ± 2	7.81 ± 0.45	0.63 ± 0.01	3.03 ± 0.14	2.79 ± 0.14	

[a] Averaged over five devices with the indicated error range corresponding to the standard deviation.
[b] 0.94 correction factor was applied to PCE on the basis of the spectral mismatch.

#133177 - $15.00 USD Received 10 Aug 2010; revised 9 Sep 2010; accepted 10 Sep 2010; published 17 Sep 2010

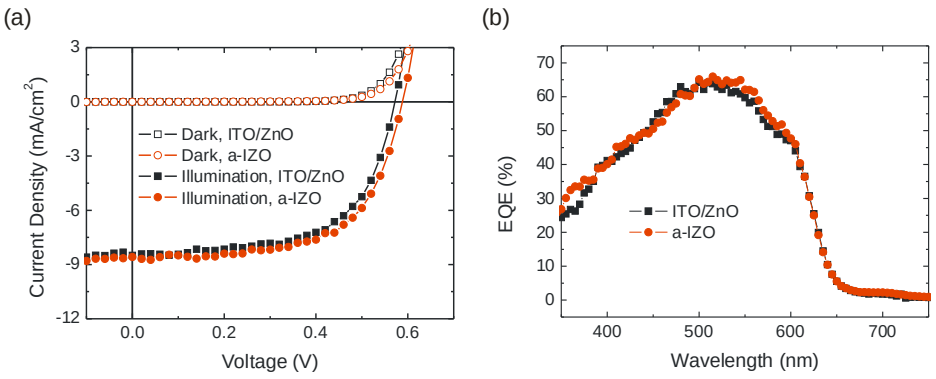

Fig. 3. (a) *J-V* characteristics and (b) EQE (%) for best inverted devices with the structures of *a*-IZO/P3HT:PCBM/PEDOT:PSS/Ag and ITO/ZnO/P3HT:PCBM/PEDOT:PSS/Ag.

Table 1 provides values of the photovoltaic performance averaged over five devices of each type. Devices with the *a*-IZO electrode exhibit comparable values of fill-factor (*FF* = 0.62 ± 0.02), but slightly higher values of open-circuit voltage (V_{OC} = 588 ± 7 mV) and short-circuit current (J_{SC} = 8.58 ± 0.15 mA/cm^2), relative to the reference devices, so that the *a*-IZO-bearing devices possessed slightly higher values of power conversion efficiency (*PCE* = 3.11 ± 0.12%). Based on the EQE spectra shown in Fig. 3b, a spectral mismatch factor of 0.94 was calculated for our devices illuminated with our solar simulator [5]. Corrected power conversion efficiency values for AM1.5 illumination based on corresponding adjustments made to the photocurrent are summarized in Table 1. Devices with the *a*-IZO electrode did not exhibit the s-shape kink in the *J-V* characteristics, nor did the reference devices with ITO/ZnO electrodes used in our study. This is in contrast to previosuly reported inverted solar cells with ITO/ZnO electrodes [8] and ITO/Al_2O_3 electrodes [5]. Studies of the electrical properties of our devices with ITO/ZnO electrodes as a function of the thickness of the ZnO layer, have shown that the s-shape kink is not observed in devices when the ZnO layer grown by atomic layer deposition is 10 nm-thick or thicker. Details of these studies will be published elsewhere [22].

4. Conclusions

In summary, we have studied the structural, optical, and electrical properties of amorphous indium zinc oxide (*a*-IZO) films deposited by RF sputtering at room temperature in a low-oxygen, argon-based atmosphere. A 200-nm-thick *a*-IZO film possessed a high optical transmittance, a low resistivity of 3.3 × 10^{-4} Ωcm, an extracted sheet resistance of about 18 Ω/□ (to be compared with the commercial ITO with sheet resistance of 15 Ω/□ at a thickness of 150 nm), and a low surface roughness (RMS) of 0.68 nm. The low work function (4.46 ± 0.02 eV) of *a*-IZO allowed for the fabrication of an inverted structure without the need of a buffer material to modify the work function. Inverted solar cells with the structure of *a*-IZO/P3HT:PCBM/PEDOT:PSS/Ag exhibited a *PCE* of 3% estimated for AM 1.5G, 100 mW/cm^2 illumination, which was comparable with reference devices using ITO/ZnO/P3HT:PCBM/PEDOT:PSS/Ag.

Acknowledgment

This material was funded in part through the Center for Interface Science: Solar Electric Materials, an Energy Frontier Research Center funded by the U.S. Department of Energy, Office of Science, Office of Basic Energy Sciences under Award Number DE-SC0001084, by the STC Program of the National Science Foundation under Agreement No. DMR-0120967, by AFOSR (BIONIC Center grant No. FA9550-09-1-0162) and by the Office of Naval Research (Grant No. N00014-04-1-0120). This work was performed in part at the

Microelectronics Research Center at Georgia Institute of Technology, a member of the National Nanotechnology Infrastructure Network, which is supported by NSF (Grant No. ECS- 03-35765). The authors would like to thank Prof. Seth Marder for providing access to his AFM system.

#133177 - $15.00 USD Received 10 Aug 2010; revised 9 Sep 2010; accepted 10 Sep 2010; published 17 Sep 2010